

# Engineering Notes

ENGINEERING NOTES are short manuscripts describing new developments or important results of a preliminary nature. These Notes cannot exceed 6 manuscript pages and 3 figures; a page of text may be substituted for a figure and vice versa. After informal review by the editors, they may be published within a few months of the date of receipt. Style requirements are the same as for regular contributions (see inside back cover).

## Lunar Base for Mars Missions

Christian Circi\*

University of Rome “La Sapienza,” 00184 Rome, Italy

### Introduction

HUMAN missions to Mars are the challenge of the 21st century, and missions with ever-increasing complexity are planned to give more information about Mars and its environment. In January 2004 two NASA rovers, Spirit and Opportunity, landed on Mars surface, and each rover carried sophisticated instruments. At the same time the ESA spacecraft, Mars Express, orbits around Mars and over several years will survey the entire planet in unprecedented detail, mapping the surface and analyzing the thin carbon-dioxide-rich atmosphere. For the next two-and-a-half decades, many NASA and ESA missions are scheduled with the goal of a human mission in 2030. Typical spacecraft mass for a Mars mission is about 1000–2000 kg, whereas human missions, or a cargo mission, require a bigger total mass, and because of the large Earth gravitational constant the spacecraft is assembled in low Earth orbit rather than on the Earth surface. Vadali et al.<sup>1,2</sup> show that for 525,000 kg as initial mass in a circular parking orbit at 1200-km altitude the payload mass in a circular synchronous orbit around Mars (orbit of six Mars radii) is 40,000 kg for a 145-day transfer time and 70,000 kg for a 168-day transfer time. The result is caused principally by the fact that half of the initial mass is used to escape from the Earth gravity field. In nominal configuration performances of the European launcher Ariane 5 for final circular orbit at 1200-km altitude, the mass is approximately 18,000 kg,<sup>†</sup> and for 525,000 kg of payload 30 missions are required. For 2024 a human mission to the moon is scheduled to show the key life support and the habitation technologies, as well as the aspects of crew performance and adaptation and in situ resources utilization technologies. In fact, before the Mars adventure it is necessary to study permanent human mission on the moon, and innovative lunar base designs have been presented emphasizing the architecture to design novel base concepts.<sup>3</sup> This Note studies the performances for direct moon–Mars transfer and analyzes the advantage of using the moon as initial launch base. The first section studies the launcher ascent trajectory from the lunar surface to low moon orbit. Because of the low moon gravitational constant and the absence of atmosphere, the ascent trajectory gives high performance with respect to the Earth case. The second section studies the escape from the Earth-moon system. The trajectory is considered as a four-body problem, and the influence of Earth, moon, and sun are taken into account to reduce the propellant mass requirement. The

third section studies the interplanetary trajectory and the insertion maneuver into a synchronous Mars orbit. The range of launch dates considered is 2025–2035, and the thrust steering for the minimum propellant mass consumption is found by using the calculus of variations. The propulsion system used is a low-thrust engine where the exhaust velocity can be modulated.

### Ascent Trajectory from the Lunar Surface

The payload mass is maximized by using a two-stage launcher with solid propellant. The absence of the atmosphere makes it possible to avoid the gravity-turn phase, and after the liftoff and the pitch-over maneuver the first stage immediately begins the guided phase. For guided phase the Q guidance, introduced by Battin and based on the velocity-to-be-gained concept, is used.<sup>4</sup> A typical optimization problem for launcher ascent trajectory consists of payload-mass maximization. The initial and the final conditions, respectively, the launch base latitude and longitude and the final orbit parameters, are considered as boundary constraints and the launcher characteristics [total mass, thrust magnitude, specific impulse, geometrical dimension, lift and drag coefficients as a function of Mach number and angle of attack, fairing mass, maximum dynamic pressure, maximum  $q \cdot \alpha$  (where  $q$  is the dynamic pressure and  $\alpha$  is the angle of attack), maximum aerothermal flux after separation of the heat shield] as input values. Key parameters for the ascent trajectory (the azimuth angle, the pitch angle, the pitch-over maneuver length, the coasting time, the variables for guided phase) are matched to satisfy all boundary and path constraints to maximize the payload mass. In the present case the inverse problem is studied: the payload mass is fixed, and the optimization process minimizes  $m_1$  and  $m_{11}$ , respectively the first- and second-stage mass. The saved propellant during the ascent trajectory is added to the initial payload mass. Data from Refs. 5 and 6 are used to design the launcher: thrust-to-weight ratio  $T/m_0 g_0 = 1.3$ , where  $m_0$  is the total mass (kilograms) and  $g_0 = 9.81 \text{ m/s}^2$ ; engine specific impulse  $I_{\text{sp}} = 300 \text{ s}$ ; and structural factor  $\varepsilon = 0.1$ . The variables of the optimization problem are the first-stage mass  $m_1$ , the second-stage mass  $m_{11}$ , the azimuth angle, the pitch angle, the pitch-over maneuver length, the coasting time between the first and second stage, and the variables for Q-guidance phase. The launch base is assumed equatorial and the final orbit circular at 200 km altitude. Table 1 shows the optimization process results. The launcher is composed of a large first stage, and only a small second stage is necessary to complete the mission. During the first part of the ascent trajectory, after the liftoff and the pitch-over maneuver, the guided phase immediately reduces the flight-path angle to reduce the gravitational loss as soon as possible. The complete ascent trajectory is composed of a coasting arc between the first- and second-stage thrust phase (like a Hohmann transfer). Note that, in nominal configuration the Ariane 5 total weight is 710,000 kg, whereas in this case the total launcher mass is only 459,146 kg.

Received 13 July 2004; revision received 6 October 2004; accepted for publication 6 October 2004. Copyright © 2004 by the American Institute of Aeronautics and Astronautics, Inc. All rights reserved. Copies of this paper may be made for personal or internal use, on condition that the copier pay the \$10.00 per-copy fee to the Copyright Clearance Center, Inc., 222 Rosewood Drive, Danvers, MA 01923; include the code 0731-5090/05 \$10.00 in correspondence with the CCC.

\*Assistant Professor, Department of Aerospace and Astronautical Engineering, Scuola di Ingegneria Aerospaziale, via Eudossiana 16.

<sup>†</sup>Data available online at [http://www.arianespace.com/site/documents/ariane5\\_man\\_index.html](http://www.arianespace.com/site/documents/ariane5_man_index.html) [cited 6 July 2004].

Table 1 Ascent trajectory performance

Parameter	Mass, kg
Stage I	234,881
Stage II	3,725
Payload	220,540
Total mass	459,146

## Escape from the Earth–Moon System

During the escape phase from the Earth–moon system, the trajectory is considered as a four-body problem, and both Earth and sun gravity-gradient effects are taken into account. To receive the maximum Earth gravity-gradient help, the transfer orbit apocenter must be toward the external collinear Lagrange point  $L_2$  of the Earth–moon system. This allows the minimum escape eccentricity with respect to the moon, or rather the minimum eccentricity necessary to open the zero-velocity curves (ZVC) at  $L_2$ . The ZVC are closed at  $L_2$  only if the value of the Jacobi constant is more negative than  $C_2$  (the value of the Jacobi constant at the  $L_2$  Lagrange point) and because these curves act as a barrier the spacecraft cannot escape from the moon.<sup>7</sup> After escape from the moon gravity field, to receive the sun gravity-gradient help it is necessary for the spacecraft trajectory to be along the sun–earth radial line. This synchronization allows escape from the Earth–moon system with only one impulse given at the initial low moon orbit. The minimum  $\Delta V$  necessary to escape from the moon gravity field is also strong enough to allow escape from the Earth–moon system. The  $\Delta V$  from the initial circular orbit to the escape trajectory is 614 m/s, the eccentricity with respect to the moon equal to  $e = 0.92$ , and the transfer time to the Earth sphere of influence is 35 days. With structural factor  $\varepsilon = 0.1$ ,  $I_{sp} = 350$  s, and an initial mass of  $m_i = 220,540$  kg, the payload mass at the

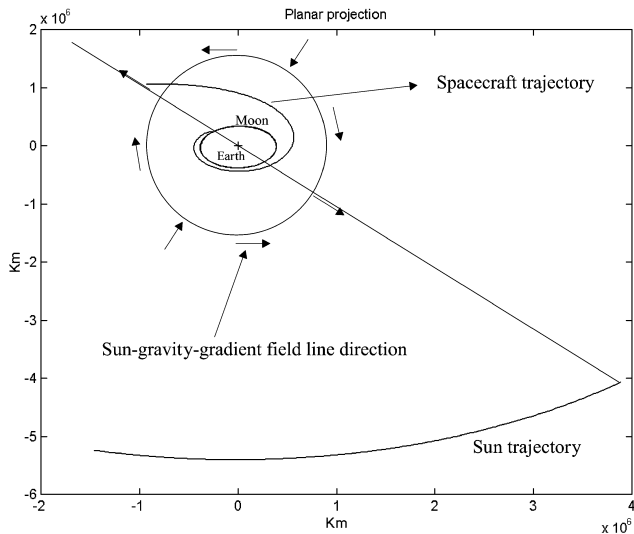


Fig. 1 Numerical escape trajectory from Earth–moon system.

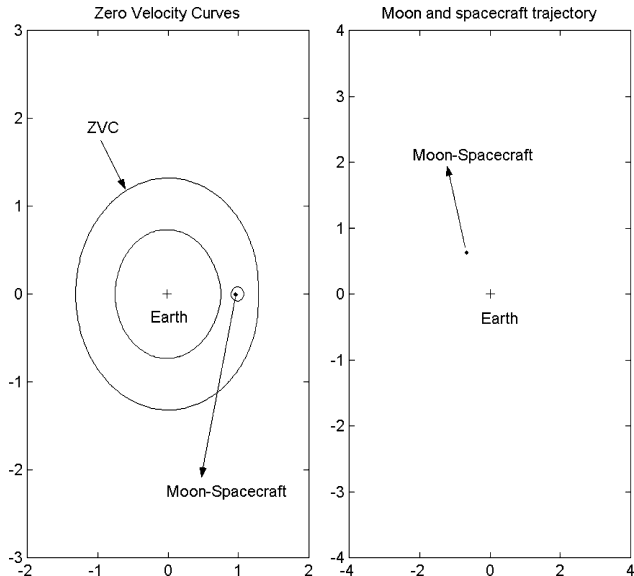


Fig. 2 ZVC at the beginning of the mission.

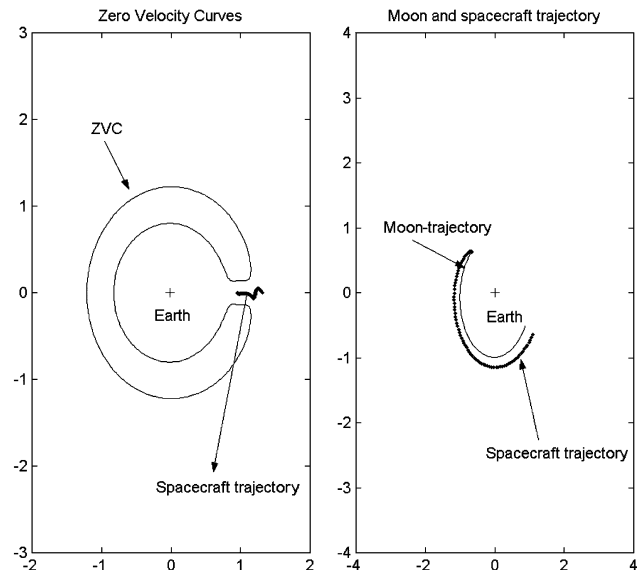


Fig. 3 ZVC at the escape point.

beginning of the heliocentric trajectory is 180,413 kg. Note that if this maneuver is given directly by the launcher additional mass can be saved. Figure 1 shows, in the inertial Earth-centered frame, the numerical trajectory by using planetary ephemerides. (The sun trajectory is scaled.) The spacecraft escapes from the Earth–moon system through the radial position using the sun gravity-gradient effect, and the minimum escape eccentricity from the moon allows escape also from the Earth–moon system without additional maneuvers. Figures 2 and 3 show the ZVC shape (left-hand sides) and the moon and spacecraft trajectory in the inertial Earth-centered frame (right-hand sides), for two different times, at the beginning of the trajectory (Fig. 2) and at the escape point from the Earth–moon system (Fig. 3). At the beginning the ZVC are closed around the spacecraft, and because the ZVC act as barriers for the motion the spacecraft cannot escape from the moon. During the trajectory, small perturbations, caused by the moon eccentricity and solar gravity field,<sup>8</sup> increase the Jacobi constant value and open the ZVC allowing escape.

## Interplanetary Transfer and Insertion Trajectory into a Mars Synchronous Orbit

A low-thrust engine, where the exhaust velocity can be modulated, is preferred to chemical propulsion, and the optimal thrust acceleration is obtained from the calculus of variations.<sup>9</sup> The engine input power, specific mass, and efficiency of the powerplant, as used in Refs. 1 and 2, are 10 MW, 6 kg/kw, and 0.6, respectively. The heliocentric transfer trajectory is a rendezvous problem between the initial point, close to sun–Earth  $L_2$  Lagrangian point, and the final position and velocity of Mars. The rendezvous problem with minimum-fuel expenditure is solved by using a “hybrid” direct/indirect method. A direct method that minimizes the performance index by making appropriate changes to the control history and an indirect method to satisfy the necessary conditions are combined to form the hybrid nonlinear programming method.<sup>10</sup> The results are departure date 6 December 2028, transfer time to Mars sphere of influence 195 days, and final mass 150,389 kg.

The insertion maneuver into a circular synchronous Mars orbit is studied starting from the position and velocity values at the Mars sphere of influence, obtained from the rendezvous problem. The flight time is five days, and the final mass 124,639 kg. Because the specific mass of the powerplant is assumed to be 6 kg/kw, the mass of the 10 MW of powerplant is 60,000 kg, and the final payload mass in a synchronous Mars orbit is 64,639 kg. Note that a similar payload mass is obtained using direct Earth–Mars trajectories with 30 missions of the Ariane 5 launcher, whereas using moon–Mars trajectories only one mission is required.

## Conclusions

A lunar base for permanent human mission in space is demonstrated to be very useful also as initial base of launch for direct moon–Mars missions. Starting from the lunar surface, a total launch vehicle mass of 459,146 kg, using the sun and Earth gravity-gradient effect and a low-thrust exhaust-modulated propulsion system, reaches a synchronous Mars orbit with a 64,639-kg payload. Using direct Earth–Mars transfer, half of the initial mass is needed to escape from the Earth gravity field, and 30 missions of the Ariane 5 launcher are required to obtain the same payload for synchronous Mars orbit. Transfer to Mars via the moon is very advantageous with respect to classical direct Earth–Mars missions and gives a good opportunity for future Mars exploration.

## Acknowledgment

The author gratefully acknowledges F. Graziani for comments and suggestions.

## References

- <sup>1</sup>Vadali, S. R., Nah, R., Braden, E., Johnson, I. L., Jr., “Fuel-Optimal Planar Earth-Mars Trajectories Using Low-Thrust Exhaust-Modulated Propulsion,” *Journal of Guidance, Control, and Dynamics*, Vol. 23, No. 3, 2000, pp. 476–482.
- <sup>2</sup>Vadali, S. R., Nah, R., and Braden, E., “Fuel-Optimal, Low-Thrust, Three-Dimensional Earth-Mars Trajectories,” *Journal of Guidance, Control, and Dynamics*, Vol. 24, No. 6, 2001, pp. 1100–1107.
- <sup>3</sup>Lunar Design Workshop, ESA-ESTEC, Noordwijk, The Netherlands, June 2002.
- <sup>4</sup>Battin, R. H., *An Introduction to the Mathematics and Methods of Astrodynamics*, AIAA Education Series, AIAA, New York, 1987, pp. 7–14.
- <sup>5</sup>Miele, A., Wang, T., and Mancuso, S., “Assessment of Launch Vehicle Advances to Enable Human Mars Excursions,” *Acta Astronautica*, Vol. 49, No. 11, 2001, pp. 563–580.
- <sup>6</sup>Miele, A., and Wang, T., “Multiple-Subarc Gradient-Restoration Algorithm, Part 2: Application to a Multistage Launch Vehicle Design,” *Journal of Optimization Theory and Application*, Vol. 116, No. 1, 2003, pp. 19–39.
- <sup>7</sup>Szebehely, V., *Theory of Orbits*, Academic Press, New York, 1967, pp. 159–191.
- <sup>8</sup>Circi, C., and Teofilatto, P., “On the Dynamics of Weak Stability Boundary Lunar Transfers,” *Celestial Mechanics and Dynamical Astronomy*, Vol. 79, No. 1, 2001, pp. 41–72.
- <sup>9</sup>Marec, J. P., *Optimal Space Trajectory*, Elsevier Scientific, Amsterdam, 1979, pp. 53–57.
- <sup>10</sup>Dixon, L. C., and Bartholomew-Biggs, M. C., “Adjoint-Control Transformations for Solving Practical Optimal Control Problems,” *Optimal Control Applications and Methods*, Vol. 2, No. 4, 1981, pp. 365–381.